Proceedings of the 9th International Conference on Cyclotrons and their Applications
September 1981, Caen, France

BEAM INJECTION AND EXTRACTION SYSTEM FOR THE IPCR SSC

Y. Yano, N. Kishida, H. Takebe, A. Goto, T. Wada and S. Motonaga

The Institute of Physical and Chemical Research, Wako-shi, Saitama 351, Japan

Abstract.- A beam injection and extraction system for the IPCR SSC is presented. The design of the injection and extraction elements and the results of model tests are also described.

1. Beam injection and extraction system.- As to the general characteristics of the IPCR accelerator complex, see the status report presented at this conference[1]. The layout of the injection and extraction elements and their characteristics are shown in figure 1 and table 1, respectively. The latter was given by the numerical orbit calculation[2].

(i) Beam injection system.- We have made a full report on the design of the beam injection system in Ref. 3, where the beam was injected radially through one of the open valleys of the SSC. Having developed our study of the beam injection, we decided to modify the system as shown in figure 1. In this design, the beam transported from the pre-accelerators at a height of 4 m above the median plane of the SSC is injected slantingly at an angle of 45° into the central region. This vertical beam transport section consists of two 45° bending magnets (BM3 and BM2), five quadrupole magnets and steerers, making an achromatic beam transport in vertical direction possible[4]. After the vertical transport the beam is radially guided to the first acceleration orbit by means of a bending magnet(BM1), two magnetic inflection channels (MIC2 and MIC1) and an electrostatic inflection channel (EIC). We call the injection system like this "the canted injection system".

The advantages of the canted injection over the radial one are as follows; the magnetic fringe field around the sector magnets decreases so rapidly with the height from the median plane that the injected beam is affected by this field only to a small extent when it passes through the valley region. The beam focusing and steering elements can be arranged down to the central region of the SSC. In radial case, no such elements are allowed to exist along the injection trajectory through the long (∿3m) valley region where beam is being accelerated. The more spacious area is available to set the EIC in the case of canted system, because the injected beam passes over it. The circumstance that the beam line of the linac as the pre-accelerator is about 12 m higher than the median plane of the SSC (see Ref. 4) is also one of primary factors for our decision.

Besides the principal role to guide the beam onto the first acceleration orbit, the injection system must satisfy some conditions that are imposed upon the beam at the injection point. These are indispensable for one to get well-centered acceleration orbits for wide range of mass and energy, and to extract the beam efficiently. What are to be adjusted for the beam are the position and direction, the dispersion in radial direction, and beam ellipses in six dimensional phase space. The adjustment of the position and direction of the injected beam can be accomplished by the MICs and the movable EIC whose location and direction are remotely controlled. Face angles of BM1 are determined

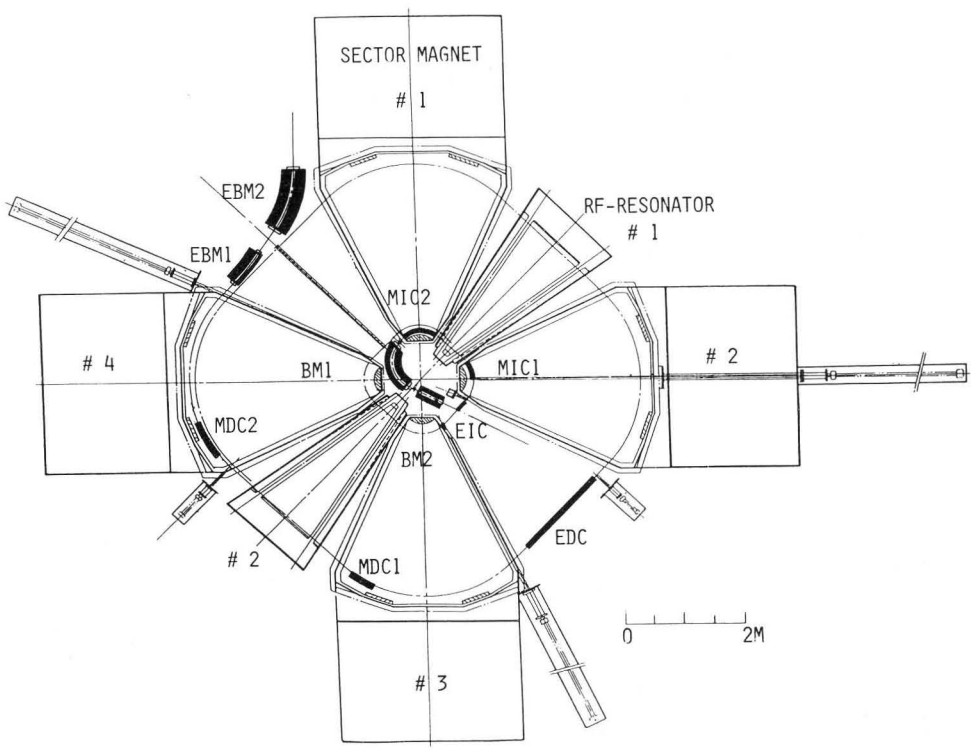

Fig. 1 : Layout of beam injection and extraction elements of the SSC.

Table 1 : Characteristics of injection and extraction elements.

Element	Bend angle(deg)	Aperture(cm) (H)	(V)	Radius(cm)	Maximum field	Face angle(deg) (entrance)	(exit)
BM2	45	4	4.2	46	17.1 kG	22.5	22.5
BM1	100	4	4.2	46	17.1 kG	14	-13
MIC2	73	4	4	43	3.3 kG	0	0
MIC1	31	3	4	50	1.3 kG	0	0
EIC	4.1	2		300	36 kV/cm		
EDC	0.79	2		linear	40 kV/cm		
MDC1	18	3	4	213	-0.5 kG	0	0
MDC2	25	3	4	230	-1.7 kG	0	0
EBM1	10	4	4.2	344	10 kG	0	0
EBM2	35	4	4	191	18 kG	0	0

so that the necessary radial dispersion of the beam may be obtained. The procedure matching the beam ellipse with the eigen-ellipse of the SSC is made by the transport system[4].

(ii) Beam extraction system.- Low-energy light ions and heavy ions can be extracted by acceleration. The beam separation of high-energy light ions due to acceleration, however, is inadequate for single turn extraction. Therefore we use the first harmonic field perturbation in order to enlarge the beam separation at the extraction point and realize the single turn extraction for these ions. In this process we do not introduce $\nu_r=1$ resonance to avoid the degradation of the beam emittance. As to the detailed study on these circumstances, see Ref. 2.

The beam, which is peeled off by an electrostatic deflection channel (EDC), is guided out of the SSC by means of two magnetic deflection channels (MDC1 and MDC2) and two bending magnets (EBM1 and EBM2).

2. Beam injection and extraction elements.- Figure 2 shows the preliminary plan for the EIC. Because of lack of space in the central region, the cathode is supported vertically by the BeO insulator. The maximum voltage of 72 kV is fed through the bottom wall of the valley vacuum chamber. We have not yet designed the EDC in detail, but the structure of SIN type[5] is under consideration. The last extraction element EBM2 is of window frame design. The description here concentrates on the bending magnets (BM2, BM1 and EBM1) and the magnetic channels (MIC2, MIC1, MDC1 and MDC2). The former elements operates in atmosphere, while the latter elements in vacuum. To reduce the outgass from the coils of magnetic channels, we are now studying to coat the coils with alumina ceramic.

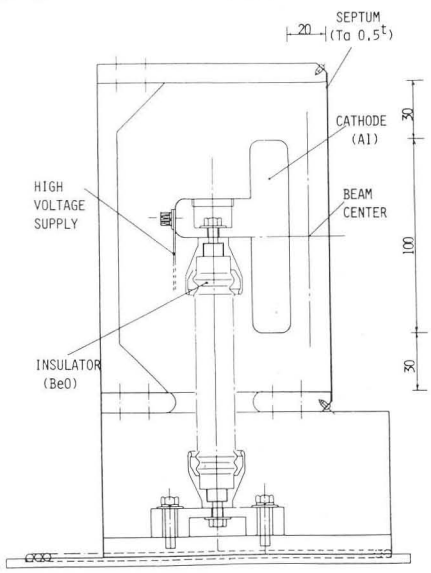

Fig. 2. : Cross-section of EIC.

(i) Bending magnets.- The injection bending magnet (BM1) is required to have the following performances: 1) It can produce the maximum magnetic field up to 17.1 kG. On the other hand, its size must be small enough that it can be set in the limited available space of the SSC central region. 2) its property in beam optics must be independent of the change of magnetic field between 6 and 17 kG to allow easy injection orbit tuning. We have designed this magnet[3] and constructed its 1/1-scale model with the bending angle of 50°. The cross section is given in figure 3. The longitudinal profile of pole edge is of Rogowski curve approximated by combining six straight lines.

The magnetic excitation curve was measured for the model magnet. The obtained magnetic efficiency was 95.4 % at 18.5 kG. While the current density ran up to 52 A/mm^2 when the magnet was excited to 18.5 kG, the maximum temperature of coils could be kept below 50°C with the water velocity of 3.9 m/sec.

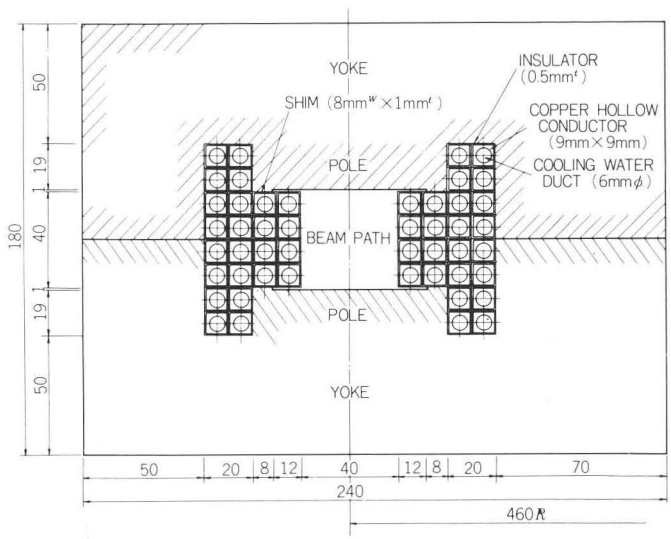

Fig. 3 : Cross-section of model bending magnet

For the detailed examination of the optical property of this magnet, the magnetic field map in the median plane throughout the beam path was measured at 7-17 kG. Figure 4 shows the magnetic field distribution in radial direction measured at θ=25°, the central position of the magnet. The uniformity better than 1×10^{-3} was obtained in -10 mm<r<+10 mm. A beam was traced through the measured field in terms of numerical orbit calculations. Because the magnet(BM1) will have the bending angle of about 90°, we have generated the magnetic field of a 90° bending magnet on the basis of the model data. In numerical calcu-

lations, a beam starts from a position 46 cm apart from one side of the magnet edges and passes through the magnet. At the starting position the beam is assumed to have phase ellipses of circular shape of 5 mm x 5 mrad in both transverse directions. The transformation of phase ellipses was calculated at exit boundary. Calculation was made for the field strength of 7 and 17 kG. Quite satisfactory results have been obtained in which the shape of ellipses were found almost same inspite of the large change of field strength. The variation of the effective boundary with change of magnetic fields was also obtained. Only change less than 130 μm was seen.

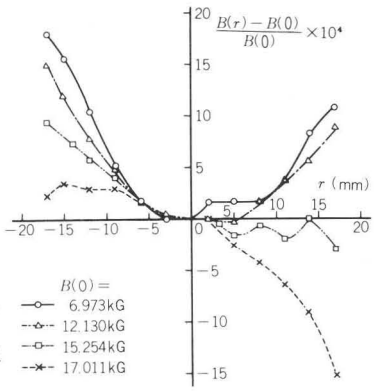

Fig. 4. Radial field distribution measured at the center of the magnet.

From the recent development in the design of vacuum chamber, it has been found that the space to install the chamber wall between BM1 and the sector magnet cannot be obtained by the structure of the model BM1. Therefore, we will remove the outer yoke and thicken the inner yoke and the upper and lower yokes. Bending magnets of the same type as BM1 are used for BM2 and EBM1.

(ii) Magnetic channels.- MIC1 and MIC2 (MDC1 and MDC2) are placed between the poles of the sector magnets and give the necessary field increase (decrease) to the sector fields along the injected (extracted) beam trajectory.

To start with, we describe about the design of MIC1 and MIC2. Two types of designs have been studied to produce the uniform field in the beam path. One type is the combination of iron shim and septum coils. This is attractive because of the advantage that the unnecessary portion in the air gap which brings about an extra ampere turns can be eliminated. This design utilizes the fact that the septum coils generate a field distribution with a sextupole component of positive sign, while the iron shims that of negative sign. We can obtain a uniform field with the combination of the shim and coils if appropriate thickness for the shim is chosen. The other type is the use of septum coils which are so designed that different current flows through the coils according as their vertical distance from the median plane. Because the coils near the median plane and those far from there generate a field distribution with a sextupole component of opposite sign to each other, we can also produce a uniform field by adjusting amounts of currents of each coils.

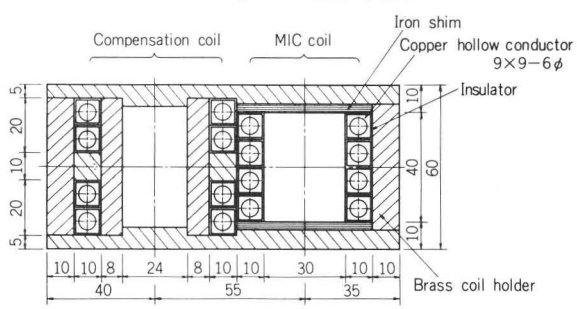

Fig. 5.: Cross-section of model MIC.

The superposition of the channel coil field onto the sector field gives rise to the undershoot in the sector field outside of the coils. To compensate for this field undershoot, another set of coils are arranged next to the MIC coils. The direction of current in the compensation coils is set opposite to that in the MIC coils. Calculations shows that the compensation coils should be wounded with the space near the median plane so as not to give extra quadrupole component to the MIC field distribution.

We have designed the MIC[6] and constructed its 1/1-scale model whose cross section is shown in figure 5. The measurement of magnetic field map inside and outside of the model MIC has been made, the model being inserted between the poles of a large H magnet with a gap of 8 cm. We have examined the combination of the shim and coils. Figure 6 shows the ratio of field increase to the base field measured for a given thickness of iron shim when the uniform field is obtained by adjusting the coil current. It was found that the field increase ratio is almost independent of the base field. From this data and the necessary field increase ratio given by the numerical orbit calculations, we can determine the thickness of iron shim necessary for each MICs as indicated in figure 6. We are now measuring the effect of compensation coils and its applicability is being confirmed.

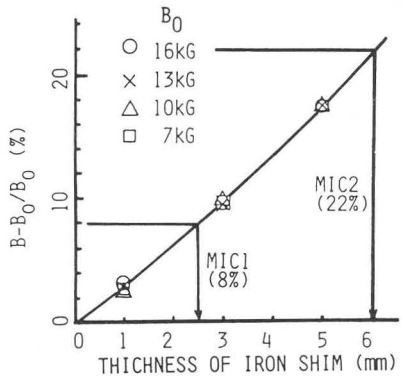

Fig. 6. : Field increase ratio $(B-B_0)/B_0$ versus a thickness of iron shim. B and B_0 represent the MIC field and the base field, respectively.

Because the MDC1 and MDC2 must reduce the sector field, the magnetic channel of the same type as MICs is inappropriate for them. We will use the septum coils mentioned above for MDCs. Their model test will start in fall of 1981.

References

1) H. Kamitsubo, IPCR SSC with K=540, this conference.
2) A. GOto et al., Calculation of injection and extraction orbit for the IPCR SSC, this conference.
3) Y. Yano et al., Sci. Papers of IPCR, 74 (1980) 13.
4) N. Kishida et al., Beam transport system for the IPCR SSC, this conference.
5) M. Olivo et al., Pro. 7th conf. on Cyclotrons and their Applications (1975) 292.
6) A. Goto et al., Sci. Papers of IPCR, 74 (1980) 124.